Investigation into the behaviour of deep beam with web openings by finite element

Jeung-Hwan Doh*[1], Tae-Min Yoo[1], Dane Miller[1], Hong Guan[1] and Sam Fragomeni[2]

[1]Griffith School of Engineering, Griffith University Gold Coast Campus, Queensland 4222, Australia
[2]School of Engineering and Science, Victoria University, Melbourne, Australia

Abstract. Currently, the design of reinforced concrete deep beams with web openings is carried out using empirical or semi-empirical methods and hence their scope of application is limited. In particular, high strength concrete deep beams with various web opening configurations have been given little treatment. In view of this, a nonlinear layered finite element method (LFEM) for cracking and failure analysis of reinforced concrete structures is used to conduct a parametric study to investigate reinforced concrete deep beams various web opening behaviours. This paper initially presents comparisons of LFEM output with published test results to numerical techniques. The paper then focuses on a parametric study on the shear strengths of deep beams with varying web opening configurations such as opening sizes and locations. The results confirm that the current design methods are inadequate in predicting the maximum shear strength when web openings are present. A series of parametric study offers insight into the maximum shear strength of the deep beams being critically influenced by the size and location of web openings.

Keywords: layered finite element; high strength concrete; deep beam; web opening; parametric study.

1. Introduction

The use of deep beams, with web openings in structural engineering practices have a major impact on the industry as evidenced by the increasing popularity of their use. Deep beams present favourable advantages, due to their non-flexural nature, which can absorb high ultimate loads and span a number of meters without the aid of additional centre columns. It is in this manner that deep beams have important applications in high rise buildings, offshore structures and foundations (Tan *et al.* 2003).

During the last several decades there has been an increased popularity for including deep beams within high-rise buildings, offshore structures and foundations. In a high rise building these beams can generally be found within the lower section of the building, particularly between the residential and office section for mixed use structures, where they are incorporated as continuous transfer girders.

Web openings may need to be created within the non-flexural nature of deep beams to accommodate for utilities such as electronic cables or air-conditioning ducts. By doing this the designer can reduce the necessary area needed for the inclusion of these utilities, thus increasing the amount of useful space within the building. However, the presence of openings induces geometric discontinuity into

---

* Corresponding author, Professor, E-mail: j.doh@griffith.edu.au

the deep beams, which only enhances the complexity of the nonlinear stress distribution over the depth of the beams (Guan and Doh 2007).

It has been found that the ultimate shear strength of the deep beams depends on the location and size of the web opening compared to the critical load path. This is due to the reduction of concrete mass acting in compression along the critical load path and openings acting as a stress raiser for shear crack propagation (Kong 1977). Due to the complex nature of these beams, most of the international engineering standards have only released design equations for solid deep beams with no web reinforcement.

The finite element method of analysis provides the engineer with the capability to analyse very complex structural systems in a much more realistic manner. The method provides for a more accurate numerical solution for concrete structures, especially if the finite element program has an appropriate element that can accurately model concrete over its entire stress range and solve problems using non-linear analysis technique. The layered finite element method is used to model the behaviour of reinforced concrete deep beams with web openings tested in this research.

This paper initially presents a brief overview of the layered finite element method (LFEM) developed by Guan and Loo (1997a, 1997b) for failure analysis of reinforced concrete deep beams with web openings. A description of the important aspects of the LFEM is given, including the geometric and material models and solution method. The LFEM is then used to conduct a comparison with published experimental results. After verification with test results, the LFEM was used to conduct a parametric study to analyse a range of concrete deep beams with various opening configurations. The parametric study focuses on the effect of varying opening locations and sizes. In total, 53 models were analysed or compared.

2. Current design formula for deep beam with web openings

Based on experimental studies, Kong *et al.* (1970, 1978) and Kong and Sharp (1973, 1977) derived design equations for normal and lightweight concrete deep beams with and without web openings. The ultimate shear strength equations for reinforced concrete deep beams are

$$Q_{ult} = C_1 \left[1 - 0.35 \frac{x}{D} \right] f_t bD + C_2 \sum A_w \frac{y}{D} \sin^2 \alpha \qquad (1)$$

for solid deep beam, and

$$Q_{ult} = C_1 \left[1 - 0.35 \frac{k_1 x}{k_2 D} \right] f_t b k_2 D + \sum \lambda C_2 A_w \frac{y_1}{D} \sin^2 \alpha_1 \qquad (2)$$

for deep beam with web opening
where the meanings of symbols are illustrated in Fig. 3. b is the width of the beam and C_1 and C_2 are the coefficients and taken as 1.35 and 300 N/mm^2, respectively, following the ASTM standard C330 which is related to the material properties for light weight concrete and reinforcement steel.

Kong and Sharp (1973, 1977) and Kong *et al.* (1978) made significant contributions to the development of the British Standard and the first term on the right side of Eq. (1) and Eq. (2) expresses the load capacity of a strut. When an opening is in the natural loading path, the first term considers the lower load path. The second term on the right side of the equation articulates the contribution of reinforcement in deep beams. It should be noted however, that these equations are

only applicable for concrete strengths less than 46 MPa.

Tan *et al.* (1995, 1997, 2003) and Leong and Tan (2003) investigated the effects of high strength, shear span to depth ratios and web reinforcement ratios of the beams using both an experimental program and numerical analysis. The design shear strength for high strength concrete deep beams is

$$V_n = \cfrac{1}{\cfrac{\sin 2\theta_s}{f_t A_c} + \cfrac{1}{f_c' A_{str} \sin \theta_s}} \tag{3}$$

where $f_t = \cfrac{2A_s f_y \sin \theta_s}{\cfrac{A_c}{\sin \theta_s}} + \cfrac{2A_w f_{yw} \sin(\theta_s + \theta_w)}{\cfrac{A_c}{\sin \theta_s}} \cdot \cfrac{d_w}{d} + f_{ct}$ and $\tan \theta_s = \cfrac{h - \cfrac{l_a}{2} - \cfrac{l_b}{2}}{a}$

Eq. (2) has limitations on the web opening size and location with respect to the x/D ratio within the 0.25 to 0.4 range. However Eq. (3) does not give any design limitations in regards to the opening size, location or orientation of the opening size; or for that fact, the geometry of the beam itself, including the x/D or L/D ratio. Either they have not considered the effect of these variables, or they are confident that the equation will work under any circumstance.

Although Yang *et al.* (2006) supports the use of these two equations for high strength concrete deep beams with web openings, the authors noted that Eq. (1) and Eq. (2) were very conservative with the increase in concrete strength, thus the design of these concrete beams is less economical. C_1 in the Eq. (1) and Eq. (2) is 0.35 in which represented semi-empirical expressions from the experiments conducted by the authors. These are located within the first half of the equation, which is a measure of the load-carrying capacity of the concrete strut of the lower path in the structural idealisation ($C_1 f_t b k_2 D$). The factor

$$\left[1 - 0.35 \frac{k_1 x}{k_2 D}\right]$$

allows for experimental observation of the way the load capacity varied with cot α, where α is the inclination of the lower load path to the horizontal. As such, the first term is a semi-empirical expression for the capacity of the lower path – the strut fails when this capacity is reached (Yoo *et al.* 2011).

The second term represents the contribution of steel reinforcement to the shear strength of the beam. In this paper the second hand term will not be modified as the structural idealisation of the steel reinforcement is considered to be appropriately dealt with in this original manifestation.

Yoo *et al.* (2011) conducted an extensive test program on high strength deep beams with various web openings. Using the test results and published data, the proposed design equations were derived for high strength concrete deep beams with web openings and is expressed as

$$V_{Flex} = 1.2\left(1 - 0.15 \cdot \left(\frac{(2k_1 + 0.10a_1)}{(2k_2 + 0.90a_2)}\right)\left(\frac{x}{D}\right) f_t b k_2 D\right) + C_2 \sum \lambda \frac{A y_1}{D} \sin^2 \theta \tag{4a}$$

for opening located in Flexural zone, and

$$V_{Rigid} = 1.1\left(1 - 0.2 \cdot \left(\left(\frac{k_1 + 0.25a_1}{k_2 + 0.15a_2}\right)\left(\frac{x}{D}\right)\right) f_t b k_2 D\right) + C_2 \sum \lambda \frac{A y_1}{D} \sin^2 \theta \tag{4b}$$

for opening located in Rigid zone.

The coefficients of the parameters (C, t_2, t_3 and t_4) are obtained by linear analysis based on least square method using numerical parametric study results for best fit (Yoo 2011). This yields for Rigid zone, C_1=1.1, t_2=0.2, t_3=-0.5 and t_4=0.3 and for Flexural zone, C_1=1.2, t_2=0.15, t_3=-0.1 and t_4=0.9.

Comparison studies (Yoo *et al*. 2011) were made between Eq. (4) and those developed by Kong and Sharp (1973, 1977) and Kong *et al*. (1978) and Tan *et al*. (1995, 1997, 2003). The findings indicated that Eq. (4) gave reliable results and may be used for the design of high strength concrete deep beams with web openings. However, the empirical design predictions, Eqs. 4(a) and (b) are derived from the test results and hence further verification is required using another tool such as FEM. These include the more comparative and parametric studies when varying the web opening sizes and locations.

2. Nonlinear layered finite element method (LFEM)

For rigorous cracking and failure analysis of reinforced concrete flat plates, a nonlinear LFEM has been developed by Guan and Loo (1997a, 1997b). Fig. 1 illustrates the concept of the degenerate shell element encompassing concrete and smeared steel layers. Elements of this type were used in the LFEM where a smeared crack approach was adopted to model cracked concrete and a strain-hardening plasticity approach was employed to model concrete compressive behaviour. The effect of
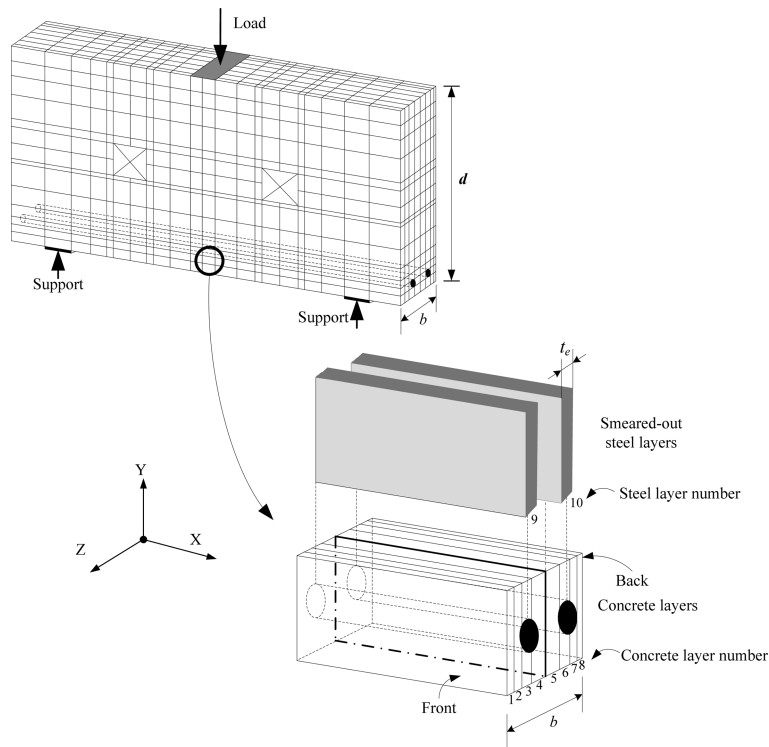

Fig. 1 Concrete and steel layers of a typical layered element

the tension-stiffening and the deterioration of shear stiffness were also considered after cracking of concrete. The contribution of the smeared reinforcing steels having elasto-plastic behaviour were added to that of concrete to form the total material constitutive matrix. With the shell element assumption, the transverse shear deformation can be accounted for, which is crucial for shear analysis (Guan and Loo 1997a, Doh *et al.* 2010).

Taking into consideration material and geometric non-linearity, the LFEM is capable of solving three-dimensional problems of reinforced concrete structures and of analysing both flexural and shear cracking up to failure. In addition, to predict the shear strength, the method is also capable of determining: the load-deflection response, the ultimate load capacity, the deformation shape and the cracking patterns of the concrete beams. It is considered far superior than the code methods and existing empirical approaches where only the shear strength can be predicted.

3. Comparison study

In order to verify the numerical modeling, previously published data on a total of forty three deep beams with various opening sizes and locations were modeled and analysed to provide an in-depth comparison study. The overall dimensions of all deep beam specimens were 2400 mm × 600 mm × 110 mm thick, as detailed in Figs. 2(a)-(c). For specimens subject to a single-point load, the shear span was 900 mm, which resulted in a clear span to depth (*l/d*) ratio of 3 and a shear span to depth ratio (*a/d*) of 1.5.
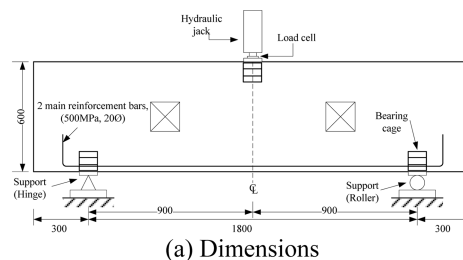

(a) Dimensions

(b) Side View

(c) Front view

Fig. 2 Loading and support conditions (dimensions in mm, Yoo *et al.* 2011)

Table 1 Web opening configuration and concrete strength

Specimens	f_c' (MPa)	Opening location (mm)		Opening size (mm)		V_{Exp} (kN)	V_{LFEM} (kN)	$V_{Eq.(2)}$ (kN)	$V_{Eq.(3)}$ (kN)	$V_{Eq.(4)}$ (kN)	$\dfrac{V_{LFEM}}{V_{Exp}}$	$\dfrac{V_{Eq.(2)}}{V_{Exp}}$	$\dfrac{V_{Eq.(3)}}{V_{Exp}}$	$\dfrac{V_{Eq.(4)}}{V_{Exp}}$
		k_1x	k_2D	a_1x	a_2D									
S01-72-1		475	270	60	60	352.8	344	110.9	155.0	157.7	0.98	0.31	0.44	0.45
S01-72-2	72	595	270	60	60	415.8	367.5	70.5	138.4	135.5	0.88	0.17	0.33	0.33
S01-72-3		355	270	60	60	422.4	362	160.0	180.8	166.6	0.86	0.38	0.43	0.39
S01-72-4		235	270	60	60	422.2	315	223.2	227.4	214.4	0.75	0.53	0.54	0.51
S02-70-1		415	330	60	60	347.7	305.5	187.5	198.9	193.1	0.88	0.54	0.57	0.56
S02-70-2	70	415	390	60	60	401.8	365.5	240.5	232.8	237.7	0.91	0.60	0.58	0.59
S02-70-3		415	210	60	60	267.9	245	77.8	127.5	121.3	0.91	0.29	0.48	0.45
S02-70-4		415	150	60	60	240.5	220	23.6	89.7	73.9	0.91	0.10	0.37	0.31
S03-63-1		505	330	60	60	303.1	263	146.7	168.5	189.0	0.87	0.48	0.56	0.62
S03-63-2	63	595	390	60	60	254.1	212	164.3	180.4	213.5	0.83	0.65	0.71	0.84
S03-63-3		325	210	60	60	189.7	204	111.0	137.1	139.4	1.08	0.59	0.72	0.73
S03-63-4		235	150	60	60	177.6	218	92.7	113.6	114.0	1.23	0.52	0.64	0.64
S04-82-1		325	330	60	60	454.2	315	240.6	246.7	234.3	0.69	0.53	0.54	0.52
S04-82-2	82	235	390	60	60	457.8	437	344.3	342.4	316.7	0.95	0.75	0.75	0.69
S04-82-3		505	210	60	60	232.3	263	49.3	128.0	111.2	1.13	0.21	0.55	0.48
S04-82-4		595	150	60	60	185.1	248	N/A*	84.4	54.7	1.34	N/A*	0.46	0.30
S05-72-1	72	415	270	60	60	309.1	300	134.3	167.0	172.1	0.97	0.43	0.54	0.56
S05-80-2	80	422.5	255	90	90	193.2	137	121.1	165.9	165.2	0.71	0.63	0.86	0.86
S05-80-3		430	240	120	120	112.8	123	103.7	155.0	152.2	1.09	0.92	1.37	1.35
S06-79-1		475	270	120	60	166.8	147.5	114.3	164.3	163.2	0.88	0.69	0.99	0.98
S06-79-2	79	595	270	240	60	122.6	137	72.5	147.6	140.1	1.12	0.59	1.20	1.14
S06-79-3		415	270	120	60	174.4	136	129.3	155.3	164.6	0.78	0.74	0.89	0.94
S06-79-4		415	270	240	60	122.8	128	129.3	155.3	138.6	1.04	1.05	1.27	1.13
S06-64-5	64	475	270	180	60	146.1	117	114.3	164.3	163.0	0.80	0.78	1.12	1.12
S06-64-6		475	270	240	60	138.2	115	114.3	164.3	162.7	0.83	0.83	1.19	1.18
S07-91-1		415	270	60	120	306.6	244	144.5	190.1	162.1	0.80	0.47	0.62	0.53
S07-91-2	91	415	270	60	180	157.9	140	144.5	190.1	163.6	0.89	0.91	1.20	1.04
S07-91-3		415	210	60	120	135.2	139	75.9	120.5	120.4	1.03	0.56	0.89	0.89
S07-91-4		415	150	60	180	111.8	130	23.4	84.3	78.0	1.16	0.21	0.75	0.70
S07-64-5	64	415	210	60	180	109.8	109	83.8	149.4	140.0	0.99	0.76	1.36	1.27
S07-64-6		415	180	60	240	81.4	92	53.6	128.5	116.8	1.13	0.66	1.58	1.44
S08-34-1		437.5	225	150	150	88.1	102	69.2	82.9	103.5	1.16	0.79	0.94	1.18
S08-34-2	34	445	210	180	180	87.0	85.5	56.5	75.9	93.8	0.98	0.65	0.87	1.08
S08-34-3		452.5	195	210	210	79.5	77	44.1	68.9	65.7	0.97	0.56	0.87	0.83
S08-34-4		460	170	240	240	72.4	71	25.3	58.1	69.8	0.98	0.35	0.80	0.96
S09-66-1		N/A				490	395	248.1	489.5	270.2	0.81	0.51	1.00	0.55
S09-66-2	66	437.5	225	150	150	125.6	102	82.0	128.6	130.2	0.81	0.65	1.02	1.04
S09-66-3		445	210	180	180	93.2	88	66.2	118.9	118.5	0.94	0.71	1.28	1.27
S09-66-4		452.5	195	210	210	78.9	76	50.7	109.2	80.9	0.96	0.64	1.38	1.02
S10-66-1		N/A				658	463	701.6	657.6	673.5	0.70	1.07	1.00	1.02
S10-66-2	66	437.5	225	150	150	583.1	275	164.0	256.7	260.1	0.47	0.28	0.44	0.45
S10-66-3		445	210	180	180	334.5	189	132.4	237.3	236.8	0.57	0.40	0.71	0.71
S10-66-4		452.5	195	210	210	174.4	188	101.3	218.0	214.2	1.08	0.58	1.25	1.23
Average											0.93	0.57	0.84	0.81
Standard deviation											0.17	0.23	0.33	0.31

*The negative strength values which indicate zero-bearing capacity
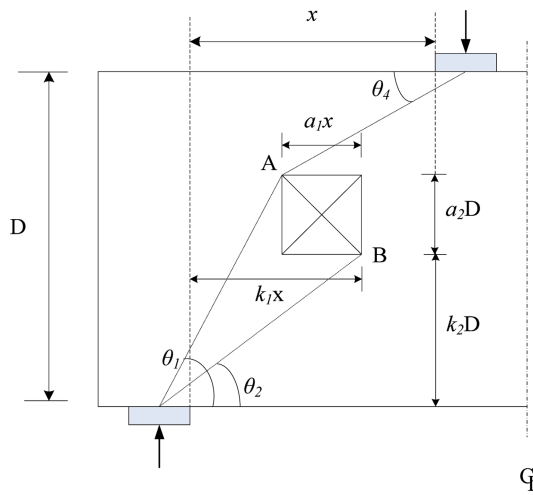
Fig. 3 Notation for size and location of opening (half length) (Kong and Sharp 1977, Yoo *et al.* 2011)

The size of openings were varied from 60 mm × 60 mm to 210 mm × 210 mm and the opening configurations for each specimen were detailed in Table 1, with details of geometric notations presented in Fig. 3. Each beam consisted of two 20 mm diameter deformed reinforcement bars, with nominal yield stress of 500 MPa, in the longitudinal direction located close to the bottom of the beam. Each bar had a length of 2700 mm and a 90 degree cog at each end with a vertical length of 200 mm to prevent end anchorage failure.

In the finite element model of the reinforced concrete deep beams with web openings, a 16 × 13 mesh was used to simulate the symmetrical half of the model (see Figs. 1 and 4(b)). Note that smaller meshes were used around the opening, the load and support regions. The mesh design was based on a convergence test (Yoo 2012) and has demonstrated to produce satisfactory numerical solution. Each beam was subdivided into eight concrete layers of varying thicknesses, while the concrete layers were thinnest for both outsides layers and gradually increased towards the mid-surface of the element. The reinforcement mesh in the wall panels was, simulated by two (smeared) steel layers.

Due to the symmetry in the geometry of the reinforced concrete wall, only half the length of the beam was considered in this study. The longitudinal reinforcements, i.e., 2N500 steel bars, are modelled as smeared steel layers with equivalent thickness.

A comparison of published test results and the LFEM output are summarised in Table 1. The results indicate that the ratios of the test to LFEM failure loads varied from 0.47 to 1.34, with a mean of 0.93 and a standard deviation of 0.17.

Eq. (2) is based on light-weight concrete deep beams, therefore its predictions are likely to produce a conservative estimation of the ultimate shear strength for the beams. Eq. (3) (Tan *et al.* 2001) also conservatively predicts the experimental results and has a high standard deviation value, which implies that the equation is not suitable for a variety of deep beam with web opening configurations. Overall the LFEM program provided a very good prediction of experimental loads.

The crack patterns of deep beams with web openings as well as the brittle failure mechanisms are reasonably predicted by LFEM. Fig. 4 shows a typical example of the crack patterns obtained by the LFEM. Figs. 4(a) and (b) clearly show the crack propagation from the soffit of the mid span of

(a) Experimental result   (b) LFEM prediction
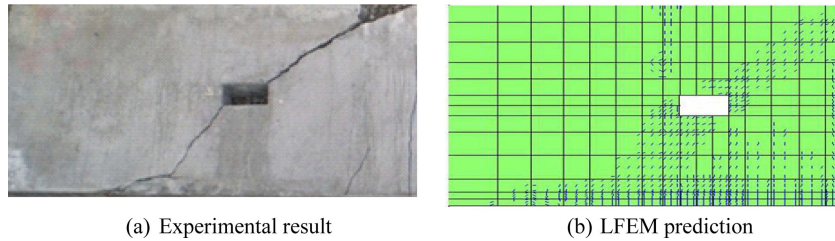
Fig. 4 Typical crack patterns of S06-79-1 (Yoo 2011) and LFEM prediction

the beams, and shear cracks, which develop diagonally from the closer edge of the rectangular opening to the support and/or loading. An observation of the actual crack mechanism in Fig. 4(a) indicates the crack pattern was reasonably well predicted. Although the test crack patterns were similar to those obtained from the LFEM, more cracks appeared in the LFEM modelling compared to the experimental test results of S06-79-1 (Yoo *et al.* 2011). The reason for this extra cracking may be that the experimental test panels exhibited more brittle material behaviour, while the LFEM predicted a less brittle behaviour due to the constitutive material modelling in LFEM. This is because in the LFEM, a crack is displayed at the any Gauss point at which the tensile strength of concrete (f'_t) is exceeded regardless of the length or width of the crack. In the experimental work, however, many of the smaller cracks are either not visible to the human eye or merge together forming a larger and more localized crack.

The vertical loads versus deflection response of typical models, predicted by the LFEM, are also compared with the experimental test results as shown Fig. 5. From these load versus deflection graphs, the LFEM results are not only able to predict the ultimate shear strength accurately but also
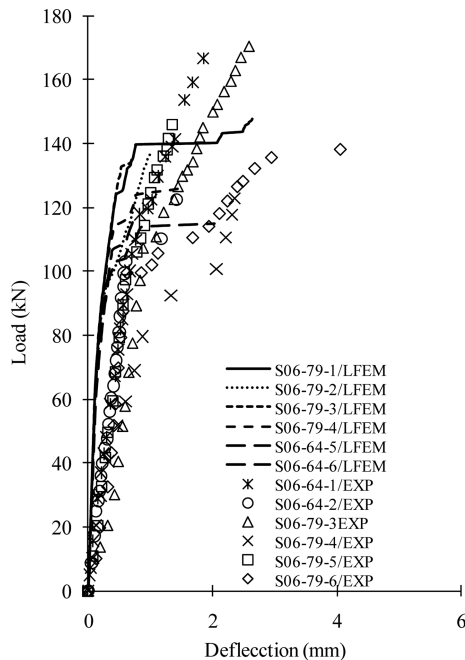

Fig. 5 Typical load vs deflection profiles (Yoo *et al.* 2011)

able to predict the load versus deflection relationship accurately.

The main purpose of the comparative study is to verify the accuracy and applicability of the LFEM model for use as an extensive and effective tool for further studies. The comparative study clearly indicates the validity of the LFEM in predicting the ultimate strength, crack propagations and deflection characteristics of high strength deep beams with various web openings. The modelling technique of the LFEM successfully adapts the geometric properties and non-linear material properties, restraint conditions and loading conditions of the test specimens conducted by previous studies. Generally, the LFEM results are presenting a close relationship for that of the ultimate loads, deflections and crack pattern predictions to the experimental results (Yoo *et al*. 2011) in a slightly conservative manner.

4. Parametric study

The LFEM has been verified to accurately predict the ultimate strength, load versus deflection response and crack propagations of normal and high strength concrete deep beams with web openings. Therefore, a series of parametric studies were performed and presented herein to investigate the effects of varying the web opening configurations.

A total of 52 LFEM models were analysed and the beams were separated into 9 groups, ensuring a variety of parameters relating to different behaviour characteristics were investigated. For each group, a minimum of five deep beam models were analysed to provide adequate data and behavioural trend. These 9 groups are categorised into 2 major parametric studies: P01 (locations) and P02 (sizes).

Details of web opening configurations for each beam are in Figs. 6 to 14 and Tables 2 to 10. The notations and geometric parameters are detailed in Fig. 3.

A total beam span and shear span to depth ratio remain constant as shown in Fig. 2. For the concrete material, compressive strength, tensile strength, Young's modulus, shear modulus and Poisson's ratio are 80 MPa, 3.58 MPa, 402038 MPa, 17516 MPa and 0.2, respectively. For the steel material, yield strength and Young's modulus is 500 MPa, 2.1×10^5 MPa, 2.3×10^4 MPa and 2.5×10^2 MPa, respectively.

For easy understanding of each deep beam design, a system of nomenclature is given as parametric

Table 2 Group 1 Specimens

Specimens	θ_1 (Rad)	θ_2 (Rad)	k_2	LFEM	Eq. (2)	Eq. (3)	Eq. (4)
P01-V-1	0.8	0.65	0.65	254.2	168.6	283	248.8
P01-V-2	0.76	0.61	0.6	238.4	147.9	263.1	225.6
P01-V-3	0.72	0.57	0.55	220.3	127.2	242.8	202
P01-V-4	0.68	0.52	0.5	200.9	106.6	222.1	178
P01-G01-1	0.63	0.47	0.45	190.2	85.9	177.6	178.5
P01-V-5	0.58	0.42	0.4	169.6	65.3	159	152.9
P01-V-6	0.53	0.36	0.35	154.8	44.6	140	127.3
P01-V-7	0.47	0.3	0.3	144.3	23.9	120.5	102.2
P01-V-8	0.41	0.24	0.25	130.1	3.3	100.3	77.7

Table 3 Group 2 Specimens

Specimens	θ_1 (Rad)	θ_2 (Rad)	k_1	LFEM	Eq. (2)	Eq. (3)	Eq. (4)
P01-H-1	0.51	0.38	0.67	233.1	57	160.9	152.1
P01-H-2	0.54	0.4	0.63	219.9	64.2	164.9	157.9
P01-H-3	0.57	0.42	0.59	195.2	71.5	169.3	164.2
P01-H-4	0.6	0.44	0.56	193.1	78.7	174.3	171.1
P01-G01-1	0.63	0.47	0.52	190.2	85.9	177.6	178.5
P01-H-5	0.67	0.5	0.48	209.8	93.1	212.3	162.7
P01-H-6	0.71	0.53	0.44	216.3	100.4	222.3	172.4
P01-H-7	0.75	0.56	0.41	229.1	107.6	233.7	182.9
P01-H-8	0.8	0.6	0.37	240.2	114.8	246.8	194.5

Table 4 Group 3 Specimens

Specimens	θ_1 (Rad)	θ_2 (Rad)	k_1	k_2	LFEM	Eq. (2)	Eq. (3)	Eq. (4)
P01-S-1	0.62	0.5	0.74	0.65	198.2	125.2	218.8	234
P01-S-2	0.62	0.5	0.69	0.6	299.2	115.4	211.1	220.2
P01-S-3	0.62	0.49	0.63	0.55	279.7	105.5	202.9	206.3
P01-S-4	0.63	0.48	0.58	0.5	232.1	95.7	194.1	192.4
P01-G01-1	0.63	0.47	0.52	0.45	190.2	85.9	177.6	178.5
P01-S-5	0.63	0.45	0.46	0.4	159.6	76.1	173.1	164.5
P01-S-6	0.64	0.44	0.41	0.35	149.9	66.3	162.7	150.5
P01-S-7	0.65	0.41	0.35	0.3	146.3	56.5	150.8	136.3
P01-S-8	0.66	0.38	0.29	0.25	144.1	46.7	136.7	122

Table 5 Group 4 Specimens

Specimens	θ_1 (Rad)	θ_2 (Rad)	k_1	k_2	LFEM	Eq. (2)	Eq. (3)	Eq. (4)
P01-P-1	0.29	0.18	0.74	0.25	229.8	N/A	89.1	54.3
P01-P-2	0.36	0.24	0.69	0.3	225.2	N/A	111.3	80.8
P01-P-3	0.44	0.31	0.63	0.35	219.9	22.9	134.5	110.3
P01-P-4	0.53	0.38	0.58	0.4	210.2	34.4	159.3	142.8
P01-G01-1	0.63	0.47	0.52	0.45	190.2	85.9	177.6	178.5
P01-P-5	0.73	0.56	0.46	0.5	195.6	117.4	241.4	192.3
P01-P-6	0.85	0.67	0.41	0.55	210.6	148.9	282.3	232.8
P01-P-7	0.96	0.78	0.35	0.6	235.4	180.4	329.9	274.2
P01-P-8	1.07	0.89	0.29	0.65	285.2	212	385.5	314.7

group followed by numeric order of models within the group.

Details of each Group specimens are shown below:

• Group 1-the location of the web opening remained at mid-depth of the beam but was moved up or down for each of the test specimens (see Fig. 6);

• Group 2-the location of the web opening remained at mid-depth of the beam, but was moved sideways for each of the allocated test specimens (see Fig. 7);

• Group 3-the location of the web opening was positioned at different locations diagonally parallel

Table 6 Group 5 Specimens

Specimens	θ_1 (Rad)	θ_2 (Rad)	a_1	a_2	LFEM	Eq. (2)	Eq. (3)	Eq. (4)
P01-G01-1	0.63	0.47	0.08	0.10	190.2	85.9	177.6	178.5
P02-G13-1	0.68	0.44	0.11	0.15	132.1	73.8	184.9	165.3
P02-G13-2	0.73	0.40	0.15	0.20	125.4	61.6	175.9	152.3
P02-G13-3	0.79	0.37	0.19	0.25	117.9	49.5	167.2	139.6
P02-G13-4	0.85	0.34	0.23	0.30	99.4	37.4	158.6	127.3

Table 7 Group 6 Specimens

Specimens	k_2	a_2	θ_2 (Rad)	LFEM	Eq. (2)	Eq. (3)	Eq. (4)
P01-G01-1	0.45	0.10	0.47	190.2	85.9	177.6	178.5
P02-G09-1	0.40	0.15	0.42	142.3	65.3	170.8	154.5
P02-G09-2	0.35	0.20	0.36	135.6	44.6	152.0	130.7
P02-G09-3	0.30	0.25	0.30	127.1	23.9	132.8	107.4
P02-G09-4	0.25	0.30	0.24	123.2	3.3	113.0	85.0

Table 8 Group 7 Specimens

Specimens	k_2	a_2	θ_1 (Rad)	LFEM	Eq. (2)	Eq. (3)	Eq. (4)
P01-G01-1	0.45	0.10	0.63	190.2	85.9	177.6	178.5
P02-G10-1	0.45	0.15	0.68	162.9	85.9	210.8	166.8
P02-G10-2	0.45	0.20	0.72	141.2	85.9	213.2	155.2
P02-G10-3	0.45	0.25	0.76	131.9	85.9	215.6	155.9
P02-G10-4	0.45	0.30	0.80	127.6	85.9	217.8	156.6

Table 9 Group 8 Specimens

Specimens	a_1	θ_1 (Rad)	LFEM	Eq. (2)	Eq. (3)	Eq. (4)
P01-G01-1	0.08	0.63	190.2	85.9	177.6	178.5
P02-G11-1	0.11	0.67	169.9	85.9	212.8	178.4
P02-G11-2	0.15	0.71	151.2	85.9	215.3	178.3
P02-G11-3	0.19	0.75	131.2	85.9	218	151.5
P02-G11-4	0.23	0.80	128.9	85.9	220.9	150.7

Table 10 Group 9 Specimens

Specimens	k_1	a_1	θ_2 (Rad)	LFEM	Eq. (2)	Eq. (3)	Eq. (4)
P01-G01-1	0.52	0.08	0.63	190.2	85.9	177.6	178.5
P02-G12-1	0.56	0.11	0.67	149.8	78.7	186.3	170.9
P02-G12-2	0.59	0.15	0.71	142.3	71.5	181.5	164
P02-G12-3	0.63	0.19	0.75	149.8	64.2	177.3	157.6
P02-G12-4	0.67	0.23	0.80	161.2	57	173.5	151.6
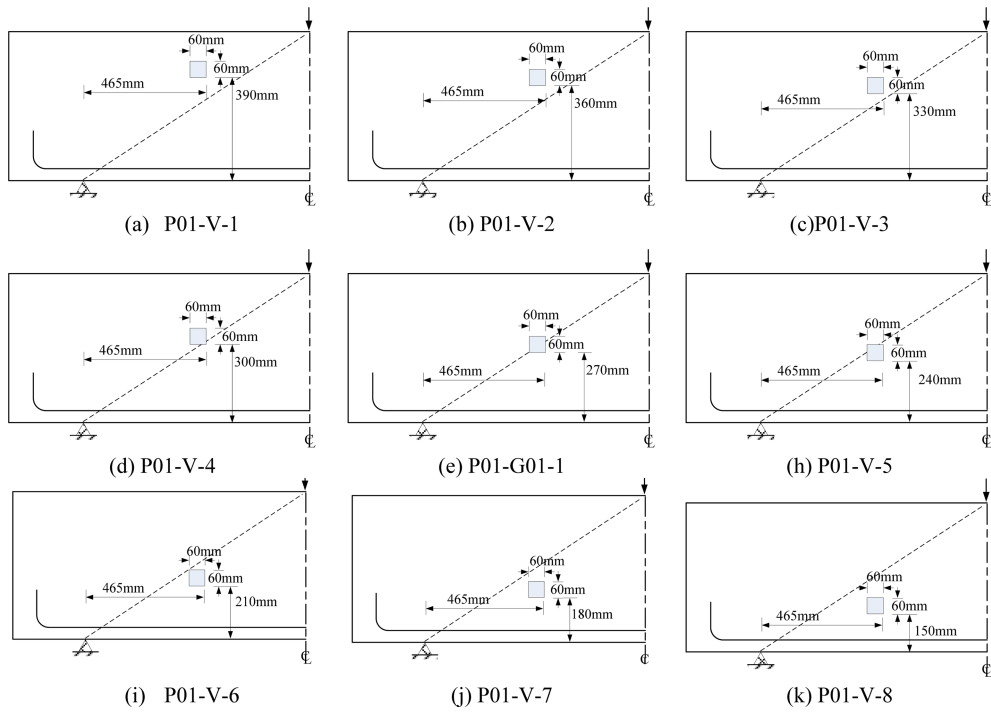
Fig. 6 Group 1 Specimens
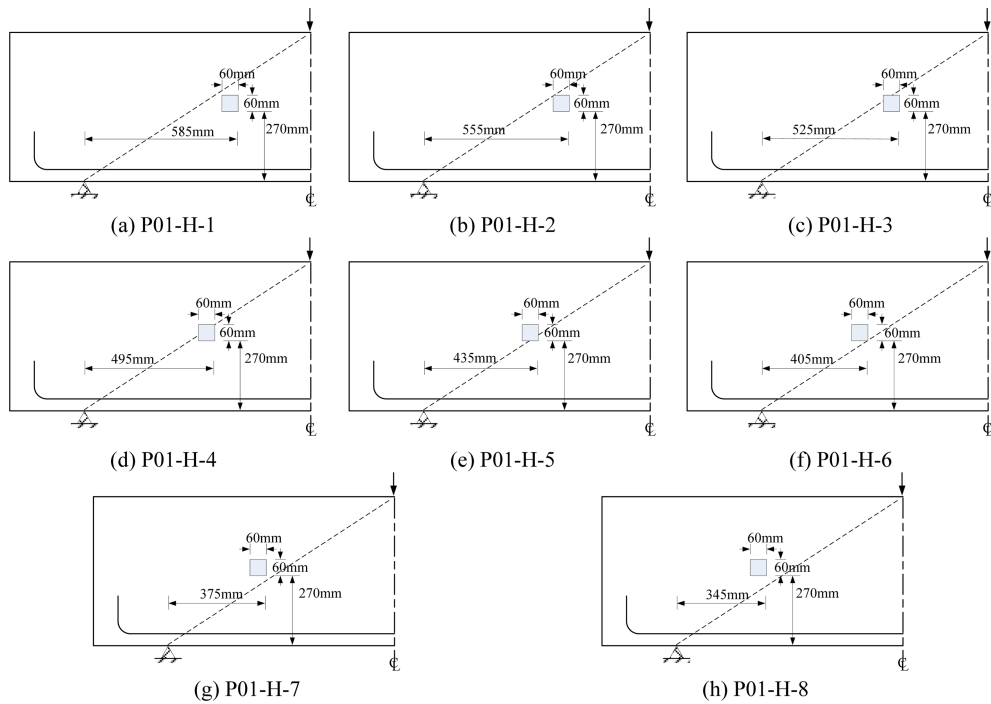
Fig. 7 Group 2 Specimens

(a) P01-S-1   (b) P01-S-2   (c) P01-S-3

(d) P01-S-4   (e) P01-S-5   (f) P01-S-6

(g) P01-S-7   (h) P01-S-8

Fig. 8 Group 3 Specimens

(a) P01-P-1   (b) P01-P-2   (c) P01-P-3

(e) P01-P-4   (f) P01-P-5   (g) P01-P-6

(h) P01-P-7   (i) P01-P-8

Fig. 9 Group 4 specimens

(a) P02-G13-1   (b) P02-G13-2   (c) P02-G13-3

(d) P02-G13-4

Fig. 10 Group 5 Specimens

(a) P02-G09-1   (b) P02-G09-2   (c) P02-G09-3

(d) P02-G09-4
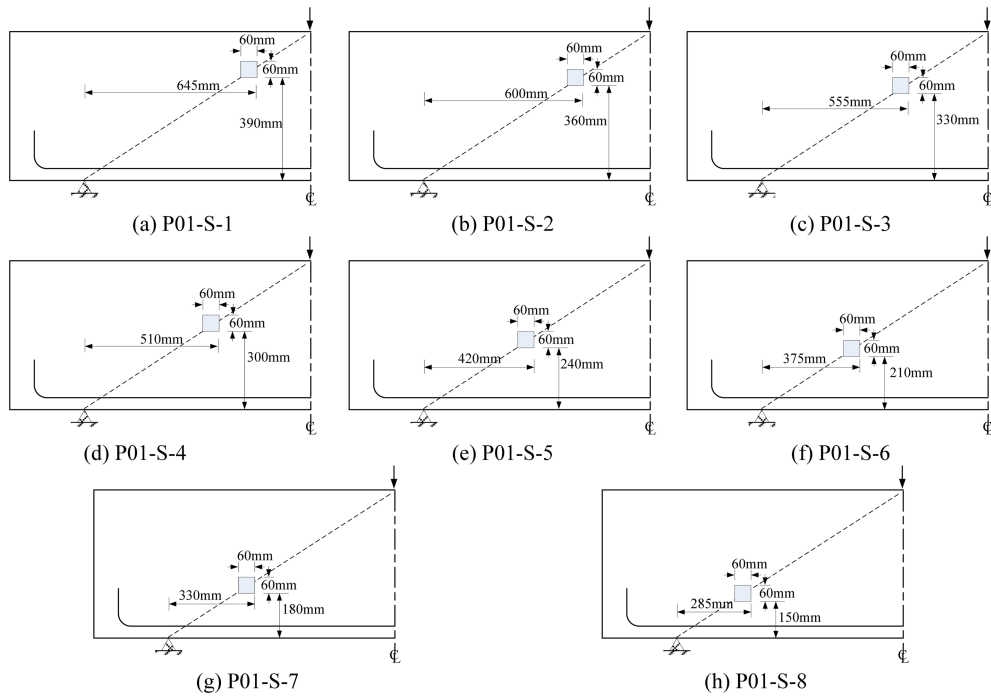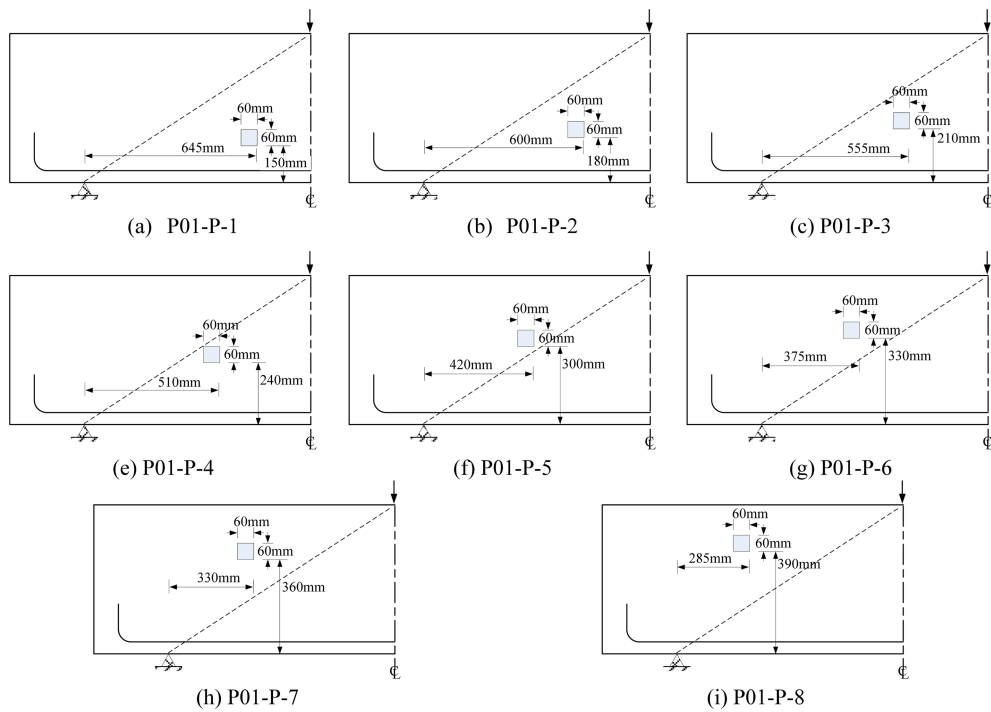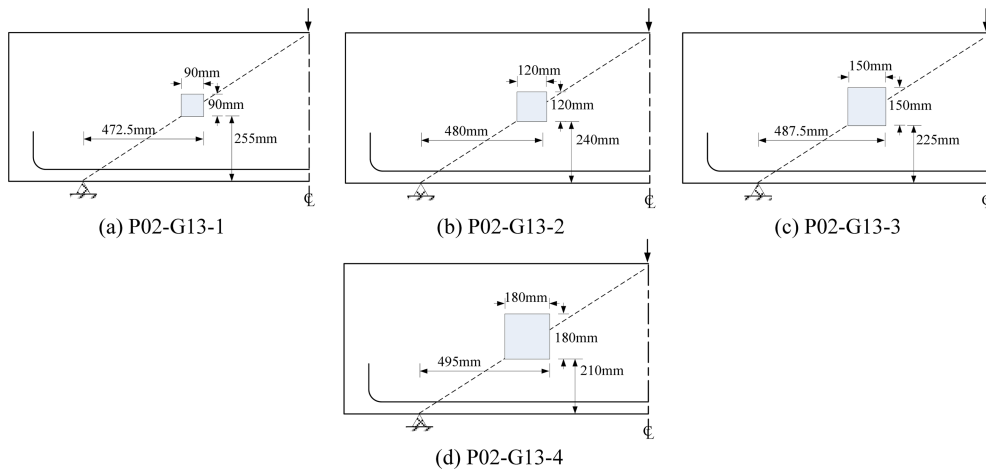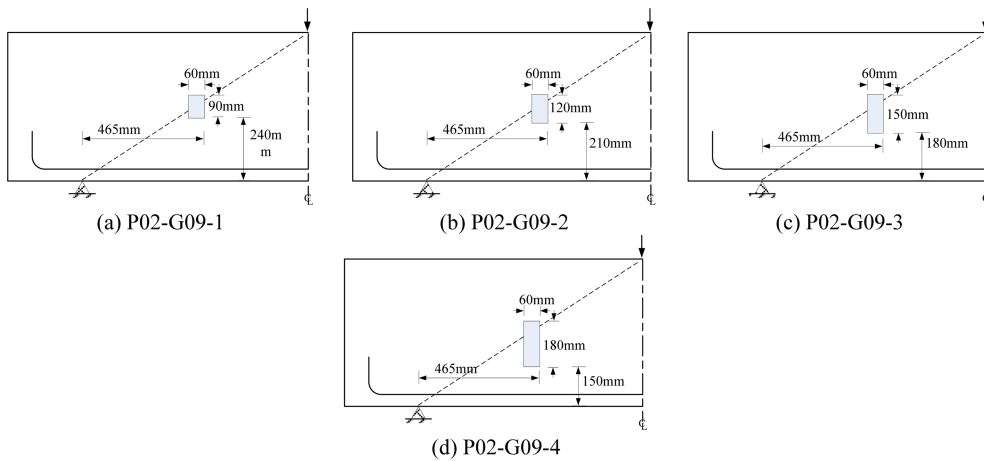
Fig. 11 Group 6

to the critical load path (see Fig. 8);
• Group 4-the location of the web opening was positioned at different locations diagonally in the beam, but perpendicular to the critical shear load path (see Fig. 9);
• Group 5-increasing web opening size. The location of the centre of the opening remained at mid-depth of the beam. Shear span to depth ratio was 1.5 (see Fig. 10);
• Group 6-the web opening was initially 60×90 mm, with increasing in depth of opening size downward (see Fig. 11);
• Group 7-the web opening was initially 60×90 mm, with increasing in depth of opening size upward (see Fig. 12);
• Group 8-the web opening was initially 60×90 mm, with increasing in the width of opening size to the left (see Fig. 13);
• Group 9-the web opening was initially 60×90 mm, with increasing in width of opening size to the right (see Fig. 14).

(a) P02-G10-1   (b) P02-G10-2   (c) P02-G10-3

(d) P02-G10-4

Fig. 12 Group 7 Specimens

(a) P02-G11-1   (b) P02-G11-2   (c) P02-G11-3

(d) P02-G11-4

Fig. 13 Group 8 Specimens

(a) P02-G12-1   (b) P02-G12-2   (c) P02-G12-3

(d) P02-G12-4
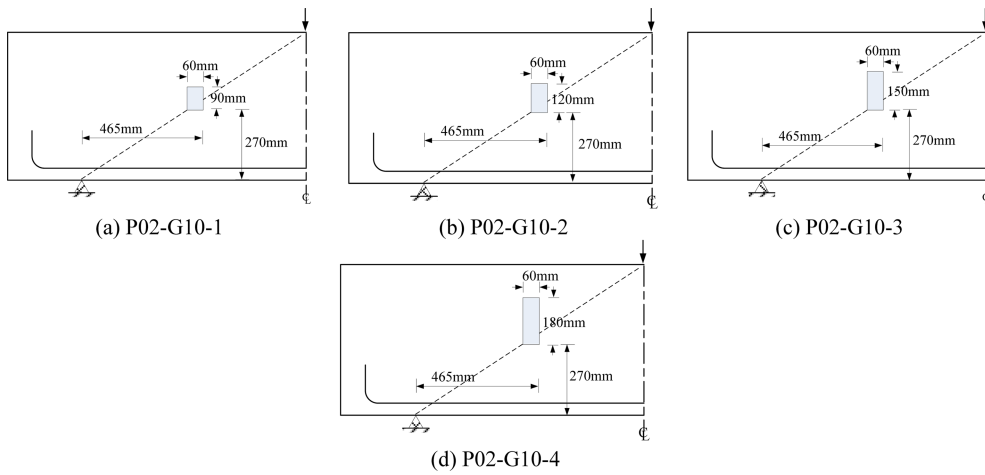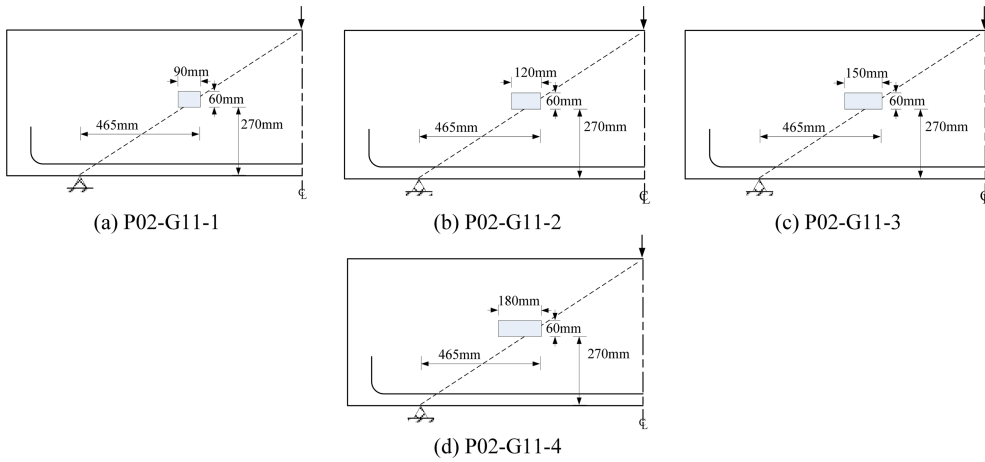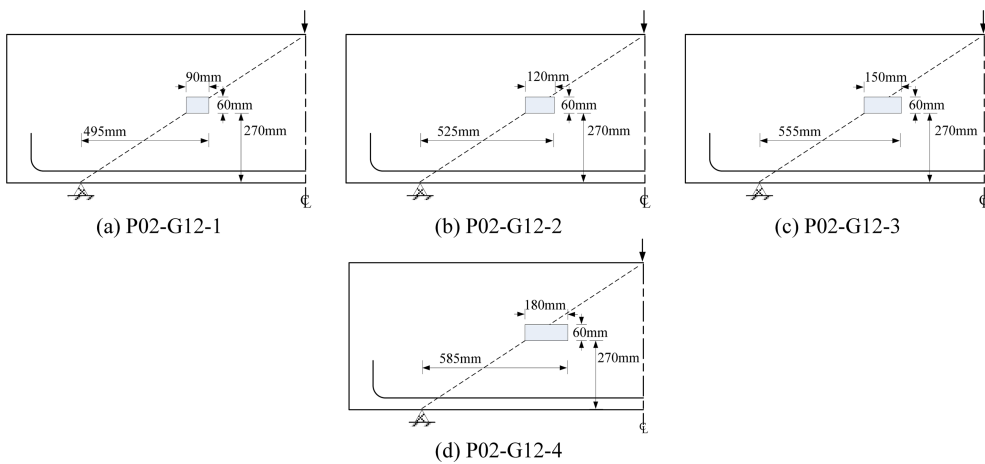
Fig. 14 Group 9

5. Results and discussion

5.1 Groups 1 and 2

Group 1 beams are designed to observe the relationship of a change in opening location in the vertical direction. Previous research suggests that as the opening moves away from the critical load path the strength of the beam will increase, this trend was also observed in the LFEM results. It can be seen from Fig. 15 that the strength of the beam decreases as the opening is moved to a lower position (Yoo *et al*. 2011).

When k_2 is increased from 0.45 to 0.65, the ultimate strength is increased from 190.2 kN to 254.2 kN. Therefore a 20% increment of k_2 results in a 34% increase of the ultimate shear strength. However, the predicted strengths by Kong *et al*. (1970) are much lower than LFEM results. Therefore the ultimate strengths predicted by Eq. (2) are too conservative. Especially the specimen P01-V-8 implying nearly zero strength as shown in Table 2. On the other hand, Eq. (3) shows the predictions are underestimated and may be unsafe where the opening's located on the rigid zone (i.e., P01-V-1 to 4). Generally, Eq. (4) gives a reliable prediction when opening is located vertically in both rigid or flexural zones.

The ultimate strength of the deep beams in Group 2 is increased until the opening is moved away from the reference location by 60 mm. However, as the opening moves further away, the ultimate strength of the beams is reduced. The ultimate strength continuously increases with the reduction of k_1. This relationship is clearly shown in Fig. 16. This is the result of the opening location varying away from the critical load path. The opening effect to the ultimate strength reduction is reduced when the opening moves within the rigid zone in the horizontal direction.

The differences between LFEM and predicted strengths using Eqs. (2)-(4) are also highlighted in Fig. 16, with both predictions indicating a significant ultimate strength decrease with an increase in
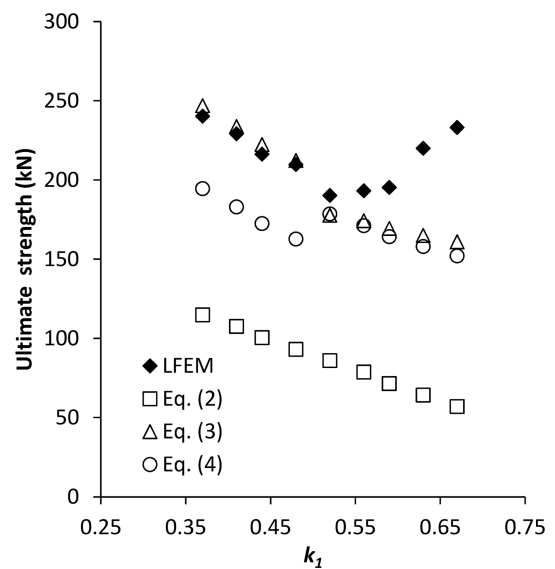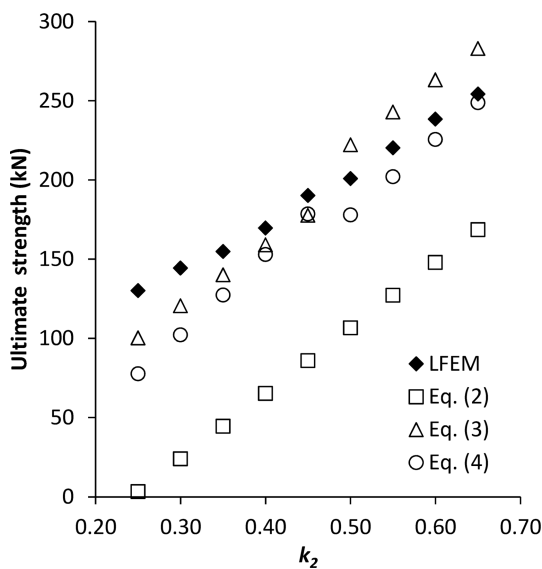

Fig. 15 Varying opening vertical position (Group 1)   Fig. 16 Varying opening in horizontal positions (Group 2)

k_1 ratio. However, this trend is not supported by the LFEM results.

The sample P01-G0-1 will be used as the baseline result for further parametric studies in the remaining groups.

5.2 Groups 3 and 4

Group 3 represents the varying of both horizontal and vertical opening location ratios, k_1 and k_2. LFEM results along with predictions are again presented in Table 4 and graphically in Fig. 17. In general, the LFEM and the ultimate strength predictions increased with the increase of k_1 and k_2. However the test ultimate strength of P01-S-1, in which the web opening is near loading zone, illustrated an unexpected different behaviour with an ultimate strength lower than that of P01-S-2. This is possibly due to the shape of the strut and the reduction effect caused by the opening. The strut is actually representative of a bottle shape with the stress from the load area spread out along the diagonal load path. When the opening is located at the neck area of the bottle shape strut, the reduction effect due to the opening is greater than when the opening is located proximate to the neutral axis of the beam. Similar outcomes were also observed by previous experimental test results (Yoo *et al.* (2011)). The predicted ultimate load capacities using Eqs. (2)-(4) are generally lower than experimental values, and increase as the web opening moves away from the soffit, even though the web opening is located close to the loading zone.

The test ultimate strengths of the Group 4 specimens are similar to each other when the openings were located above the critical zone as shown in Table 5 and indicated in Fig. 18. However, the ultimate strengths decreased significantly when openings were located in the flexural zone. The conservative nature of both Eqs. (3) and (4) were evident for the high strength concrete deep beams tested. It should be noted that Eq. (2) actually gives a negative result for the P01-P-1 and P01-P-2 implying zero strength as indicated in Table 5. This highlights the need for a modified design
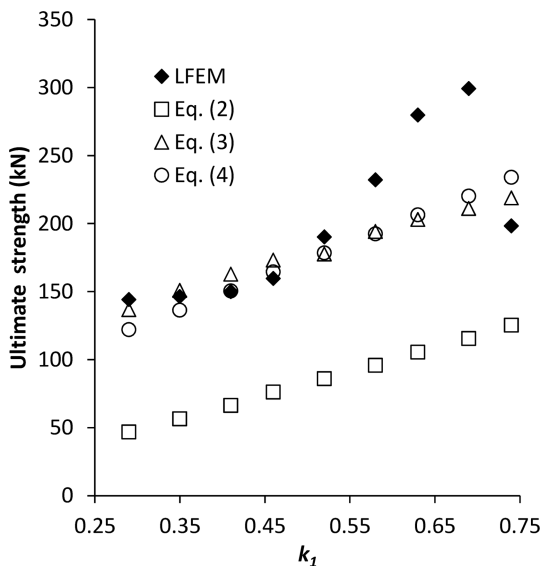
Fig. 17 Varying opening along with shear paths (Group 3)
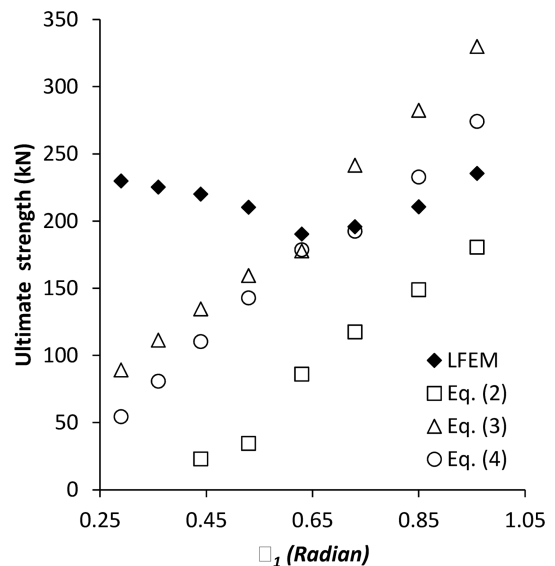
Fig. 18 Varying openings perpendicular to shear paths (Group 4)

equation to predict the maximum shear strength for such high strength concrete deep beams with openings located near the flexural zone.

5.3 Group 5

Opening size increment in both directions in Group 5 specimens results the reductions of the ultimate strength. When a_2 is increased to soffit, the ultimate strength is reduced more than when a_2 is increased to the top as presented in P02-G09 and P02-G10. However, the discrepancy is not significant and the trend of reduction of opening size increment consume when opening size is larger than 30% of the beam depth. This implies that opening size larger than 30% is not suitable for uses in practice, agreeing with the outcome of the experimental study by Yoo *et al*. 2011).

The reduction due to the opening size increment in both directions is the greatest among other opening size increment as shown in Group 5. However, the reduction of the ultimate strength due to opening size increment in both directions does not show big discrepancies with the opening size increased in vertical direction except the opening size increase to the loading point. This indicates that the ultimate strength of deep beams is not affected significantly once the opening exists.

5.4 Groups 6 and 7

Fig. 20 presents the models that are used for the parametric study P02-G09 which indicate opening size increased to the soffit of the beam vertically. The parameters which are affected by the vertical change of the web opening size are presented in Table 6, with the LFEM results. The parameters changed are k_2, a_2 and θ_2 only.

The ultimate strength is reduced with the increase of the opening size in the vertical. When the a_2 is increased from 10% to 30% vertically, the ultimate strength is reduced from 190.2 kN to 123.2 kN, which is 35% of the ultimate strength of the reference beam. However, comparing the reduction
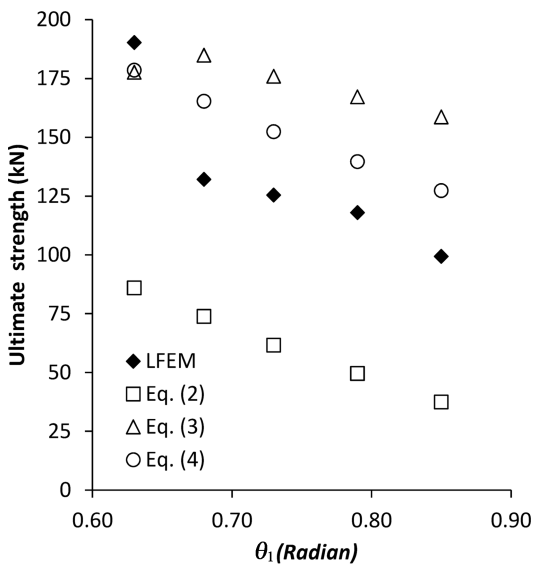

Fig. 19 Varying opening sizes (Group 5)   Fig. 20 Rectangular opening upward (Group 6)
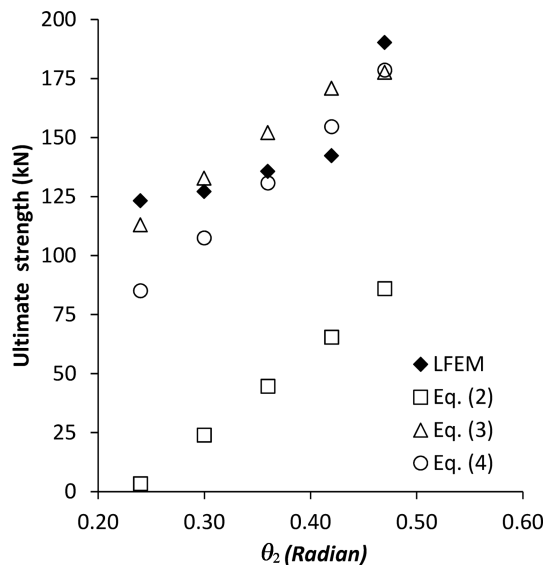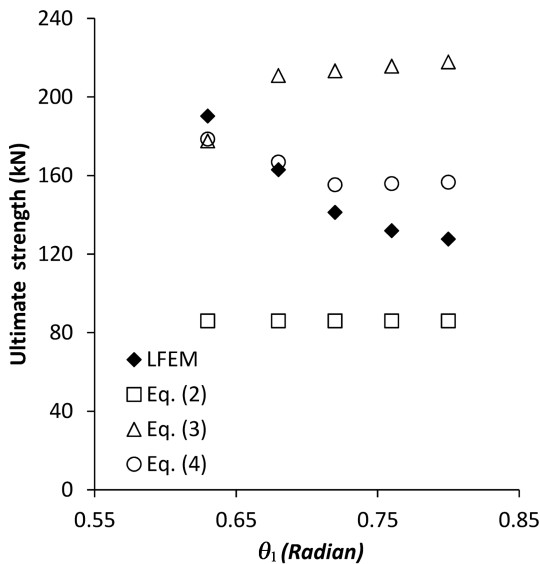
Fig. 21 Rectangular openings downward (Group 7)   Fig. 22 Rectangular openings wide left (Group 8)
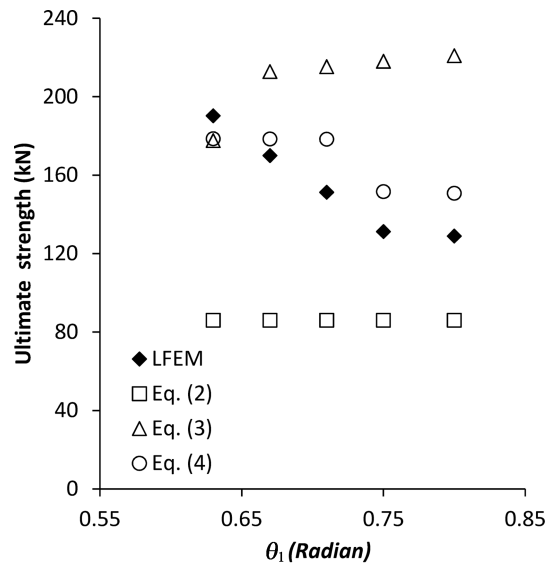
of the ultimate strength of each stage, the discrepancy in the ultimate strength is reduced even when opening size is increased consistently.

The vertical size of opening is extended upwards for Group 7 of the parametric study to investigate the effect of opening size increments on the ultimate strength. When the opening size increases from 60 mm to 90 mm, 14% of the ultimate strength is reduced. The ultimate strength is reduced by 13% when opening size is increased from 90 mm to 120 mm. These relationships are also observed in Table 8.

However the conservative nature of Eq. (2) was evident that the equation does not affect the web opening sizes varying in vertical directions. Eq. (3) shows the ultimate strength increases with the increase in web opening sizes as shown in Fig. 21. As a result, previously available design equations are not reliable and are limited in scope. Overall, Eq. (4) gives a reliable ultimate strength for the Groups 6 and 7.

5.5 Groups 8 and 9

The ratio of the ultimate strength of P02-G11-1, P02-G11-2, P02-G11-3 and P02-G11-4 to the P01-G01-1 is 89%, 79%, 69% and 67%, respectively. The lessening of the ultimate strength is reduced continuously while opening size is increased constantly into the rigid zone.

As shown in Fig. 22, opening size increment in Rigid zone affects the ultimate strength significantly and linearly until the opening size ratio a_1 becomes 0.19. When a_1 becomes 0.23, the effect from opening size increment in the horizontal direction is reduced. These indicate that as the opening size increases horizontally in Rigid zone, the relationship can be considered to be linear. As similar to Group 7 observations, both Eqs. (2) and (3) are not reliable and the applications are limited to the design of such deep beams with web openings.

The effects of horizontally increasing the opening size incrementally toward the point of loading are investigated in the parametric study on Group 9. The opening is directly interrupting the flexural
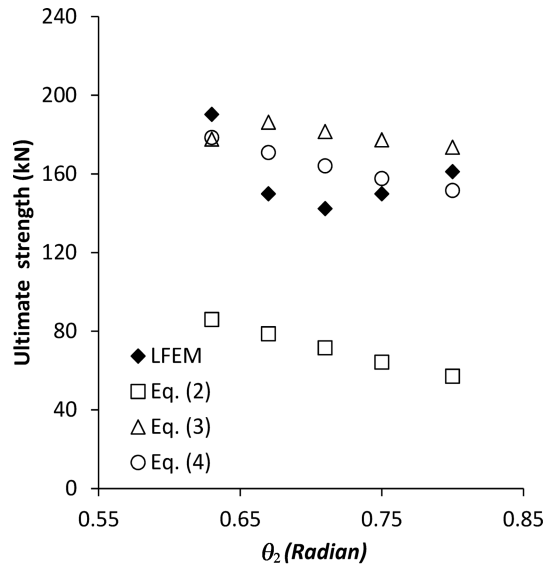
Fig. 23 Rectangular opening wide right (Group 9)

zone, which resists the bending as shown in Fig. 23.

Due to the direction of the incremental changes of the opening, k_1, a_1 and θ_1 are increased and the ultimate strength of the beam is decreased until the opening size is less than 150 mm wide, after which the ultimate strength begins to increase.

The reduction of the ultimate strength is showing similar trends with P02-G09 and P02-G10. However, when a_1 become larger than 0.15, the ultimate strength increased instead of reduced. This phenomenon is due to the flexural behaviour of specimens. Note that the increment is very small. Increment of the ultimate strength from P02-G12-02 to P02-G12-03 is 6% of the ultimate strength of P01-G01-1 and P02-G12-03 to P02-G12-04 is 7% of the ultimate strength of P01-G01-1.

6. Conclusions

The numerical investigation based on experimental data and the extension of the study is presented in this paper. With the introduction of LFEM, the comparative study with LFEM and experimental results have been completed successfully. Overall, the LFEM predicts the experimental results with greater accuracy than that of the equations presented by previous researchers. The following summaries are obtained from the 53 parametric models of high strength concrete deep beams with various geometric configurations assessed:

(1) Reducing overall size of deep beams in the same ratio in high strength concrete results in a linear reduction of the ultimate strength;

(2) When only the web opening location is changed, the ultimate strength can become higher when the opening is located closer to the top of the beam. The ultimate strength is lower when the web opening is closer to the diagonal load path;

(3) When a web opening size is extended in the vertical and, or horizontal direction, the ultimate strength of the deep beam is reduced, this reduction can be accurately described by a polynomial

relationship. However, the reduction of the ultimate strength is less when the opening size is adjusted horizontally compared to vertically.

The study found that the presence of web openings greatly change the shear strength of deep beams with various geometric configurations. Current empirical or semi-empirical design methods show varying results. Discrepancies are varied, with both conservative and unsafe results observed in the presence of web openings. In view of the significant shortcomings, there is a need to amend current design formulae and methods.

References

ACI318-08. (2008), "Building code requirements for structural plain concrete", *American Concrete Institute*, Detroit.

AS3600-2009. (2009), "Concrete structures", *Standards Australia*. Sydney, Australia.

Ashour, A.F. and Rishi, G. (2000), "Tests of reinforced concrete continuous deep beams with web openings", *ACI Struct. J.*, **97**(5), 418-426.

Doh, J.H., Guan, H. and Kim, T.W. (2010), "Parametric and comparative study of spandrel beam effect on the punching shear strength of reinforced concrete flat plates", *J. Struct. Des. Tall Spec.*, **21**(8), 605-620.

Eun, H.C., Lee, Y.H., Chung, H.S. and Yang, K.H. (2006), "On the shear strength of reinforced concrete deep beam with web opening", *Struct. Des. Tall Spec.*, **15**(4), 445-466.

Guan, H. and Loo, Y.C. (1997a), "Flexural and shear failure analysis of reinforced concrete slabs and flat plates", *Adv. Struct. Eng.*, **1**(1), 71-85.

Guan, H. and Loo, Y.C. (1997b), "Layered finite element method in cracking and failure analysis of beams and beam-column-slab connections", *Struct. Eng. Mech.*, **5**(5), 645-662.

Guan, H., and Doh, J. (2007), "Development of strut-and-tie models in deep beams with web openings", *Adv. Struct. Eng.*, **10**(6), 697-711.

Kong, F.K. (1990), "Reinforced concrete deep beams", New York: Routledge.

Kong, F.K. and Sharp, G.R. (1973), "Shear strength of lightweight reinforced concrete deep beams with web openings", *Struct. Eng.*, **51**(8), 267-275.

Kong, F.K. and Sharp, G.R. (1977), "Structural idealization for deep beams with web openings", *Mag. Concrete Res.*, **29**(99), 81-91.

Kong, F.K., Robins, P.J. and Cole, D.F. (1970), "Web reinforcement effects on deep beams", *ACI J.*, **67**(12), 1010-1017.

Kong, F.K., Sharp, G.R., Appleton, S.C., Beaumont, C.J. and Kubik, L.A. (1978), "Structural idealization for deep beams with web openings: further evidence", *Mag. Concrete Res.*, **30**(103), 89-95.

Leong, C.L. and Tan, K.H. (2003), "Proposed revision on CIRIA design equation for normal and high strength concrete deep beams", *Mag. Concrete Res.*, **55**(3), 267-278.

Mansur, M.A. and Alwis, W.A.M. (1984), "Reinforced fibre concrete deep beams with web openings", *Int. J. Cement Compos. Lightweight Concrete*, **6**(4), 263-271.

Maxwell, B.S. and Breen, J.E. (2000), "Experimental evaluation of strut-and-tie model applied to deep beam with opening", *ACI Struct. J.*, **97**(1) 142-149.

Ray, S.P. (1991), "Deep beams with web openings", *Reinforced Concrete Deep Beams*, 60-94.

Tan, K.H. and Mansur, M.A. (1992), "Partial prestressing in concrete corbels and deep beams", *ACI Struct. J.*, **89**(3), 251-262.

Tan, K.H., Kong, F.K., Teng, S. and Guan, L. (1995), "High-strength concrete deep beams with effective span and shear span variations", *ACI Struct. J.*, **92**(4), 1-11.

Tan, K.H., Lu, H.Y. and Teng, S. (1999), "Size effect in large prestressed concrete deep beams", *ACI Struct. J.*, **96**(6), 937-946.

Tan, K.H., Tong, K. and Tang, C.Y. (1997), "Effect of web reinforcement on high strength concrete deep beams", *ACI Struct. J.*, **94**(5), 572-582.

Tan, K.H., Tong, K. and Tang, C.Y. (2003), "Consistent strut-and-tie modelling of deep beams with web openings", *Mag. Concrete Res.,* **55**(1), 65-75.

Yang, K.H., Chung, H.S. and Ashour, A.F. (2007), "Influence of inclined web reinforcement on reinforced concrete deep beams with openings", *ACI Struct. J.,* **104**(5), 580-589.

Yang, K.H., Eun, H.C. and Chung, H.S. (2003), "Shear characteristics of high-strength concrete deep beams without shear reinforcement", *Eng. Struct.,* **25**(8), 1343-52.

Yang, K.H., Eun, H.C. and Chung, H.S. (2006), "The influence of web openings on the structural behavior of reinforced high-strength concrete deep beams", *Eng. Struct.,* **28**(13), 1825-1834.

Yoo, T.M. (2011), "Strength and behaviour of high strength concrete with web openings", *PhD thesis,* Griffith University.

Yoo, T.M., Doh, J.H., Guan, H. and Fragomeni, S. (2011), "Experimental behaviour of high strength concrete deep beams with web openings", *Struct. Des. Tall Spec.,* DOI: 10.1002/tal.718, 1-22.

CC